JOURNAL OF IRON AND STEEL RESEARCH, INTERNATIONAL. 2014, 21(12): 1129-1135

Effects of Hot Bending Parameters on Microstructure and Mechanical Properties of Weld Metal for X80 Hot Bends

Xu WANG[1,2], Bo LIAO[1], Da-yong WU[1], Xiu-lin HAN[2], Yuan-sheng ZHANG[3], Fu-ren XIAO[1]

(1. Key Laboratory of Metastable Materials Science and Technology, College of Materials Science and Engineering, Yanshan University, Qinhuangdao 066004, Hebei, China; 2. CNPC Bohai Petroleum Equipment Manufacture Co., Ltd., Qingxian 062658, Hebei, China; 3. China Petroleum Technology and Development Corporation, Beijing 100028, China)

Abstract: Mechanical properties of weld metal are the key factors affecting the quality of heavy-wall X80 hot induction bends. The effects of bending parameters on the mechanical properties of weld metal for hot bends were investigated by simulation conducted on a Gleeble-3500 thermal simulator. Continuous cooling transformation (CCT) diagrams of the weld metal were also constructed. The influences of hot bending parameters (such as reheating temperature, cooling rate, and tempering temperature) on the microstructure and mechanical properties of weld metal were also analyzed. Results show that the strength of all weld metal specimens is higher than the value indicated in the technical specification and increases with the increase of reheating temperature, cooling rate, and tempering temperature. The impact toughness is apparently related to the variation of reheating temperature, cooling rate, and tempering temperature.

Key words: hot induction bend; X80 steel; weld metal; heat treatment; microstructure

Bends are some of the most important accessories for long-distance gas transmission pipes[1,2]. To increase transport efficiency and decrease the pipeline construction and gas transportation costs, high-strength steel grades and/or heavy-wall pipes are applied to long-distance transmission lines[3,4], which require heavy-wall bends[2,5,6].

High-strength heavy-wall bends are usually produced from longitudinal seam submerged arc welded (LSAW) steel pipes by hot induction bending, on-line water cooling, and off-line tempering[2,5]. Although the weld metal of the LSAW is in non-deformation line, it also undergoes the same reheating, water cooling and tempering processes; therefore, the changes of the microstructure and mechanical properties of the weld metal after hot induction bending affect the bend quality. However, the chemical composition and microstructure of weld metal significantly differ from those of base metal[7], such that the variations in their microstructure and mechanical properties are different[8]. Few literature report the effects of bending process parameters on mechanical properties of the weld metal for X80 bends. Therefore, the balance of the mechanical properties of weld and base metals is crucial to the investigation of the effects of bending parameters on the microstructure and mechanical properties of weld metal.

The effects of reheating temperature, cooling rate, and tempering temperature on the microstructure and properties of weld metal for heavy-wall grade X80 bends were investigated. To understand the changing mechanism of the microstructure, continuous cooling transformation (CCT) diagrams were constructed. The difference between the microstructure transformation of weld and base metals was discussed. The results obtained will be beneficial to the production of high-performance grade X80 bends with heavy-wall thickness.

Foundation Item: Item Sponsored by National Natural Science Foundation of China (51171162); R&D Project of CITIC-CBMM (2011-D056-3)
Biography: Xu WANG, Doctor Candidate; **E-mail**: cyddjyjs@263.net; **Received Date**: December 23, 2013
Corresponding Author: Fu-ren XIAO, Professor; **E-mail**: frxiao@ysu.edu.cn

1 Experimental Materials and Procedures

1.1 Experimental materials

The chemical compositions of base metal are shown in Table 1. Steel was designed for heavy-wall X80 grade bends according to previous work[9] and manufactured into steel plates with a thickness of 25.4 mm by thermomechanical control process. The steel plates were then manufactured into 1219 mm (outer diameter) × 25.4 mm weld pipes by J-shape, C-shape, O-shape and Expanding (JCOE) forming processes and double-face tandem four-wire submerged arc welding. The chemical compositions of weld metals are also shown in Table 1. Two types of specimens were extracted from the near outside of weld metal. Firstly, square-shaped specimens with size of 10 mm × 10 mm × 80 mm were extracted from the transverse weld line; secondly, rod-shaped specimens with size of ϕ6 mm × 80 mm were extracted from the longitudinal weld line, as shown in Fig. 1.

Table 1 Chemical compositions of base and weld metals mass%

Elements	C	Si	Mn	Cr	Mo	Ni	Cu	Ti	Nb	V	P	S	P_{cm}	C_{eq}
Base metal	0.07	0.20	1.74	0.100	0.220	0.240	0.160	0.017	0.053	0.041	0.010	0.004	0.195	0.459
Weld metal outside	0.07	0.27	1.60	0.092	0.244	0.157	0.144	0.016	0.029	0.028	0.010	0.004	0.191	0.431
Weld metal inside	0.07	0.27	1.60	0.098	0.238	0.175	0.155	0.014	0.033	0.031	0.009	0.004	0.191	0.446

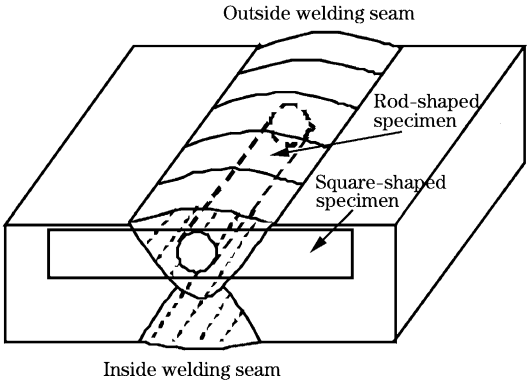

Fig. 1 Sketch map of sampling from the weld metal

1.2 Experimental procedures

Hot simulation tests were conducted on a Gleeble-3500 thermal simulator. The process parameters are as follows: the reheating time from room temperature to bending temperature ranging from 930 to 1050 ℃ was approximately 45 s, the holding time was 60 s, the cooling rate ranged from 5 to 25 ℃/s, and the tempering temperature ranged from 500 to 600 ℃. After the thermal simulation test, the tensile property and low-temperature impact toughness of the simulated specimens under different conditions were measured.

To investigate the phase transformation, the CCT diagrams of weld metal were measured by dilatability on a Gleeble-3500 thermal simulator. The specimens were austenitized at 990 ℃ for approximately 3 min and subsequently cooled down to room temperature directly with varied constant cooling rates from 0.5 to 35 ℃/s.

The microstructure observation specimens were obtained from the specimens for property tests. The microstructure of specimens was determined by optical microscopy, scanning electron microscopy (SEM), and transmission electron microscopy (TEM) to observe the microstructure and analyze the effects of different materials and processing conditions on the microstructure. For TEM observation, thin foils were prepared using a twin-jet electropolisher in a solution containing 10% perchloric acid and 90% glacial acetic acid. TEM was performed on a JEM-2010 TEM at 200 kV.

2 Results

2.1 Effects of reheating parameters on mechanical properties

Fig. 2 shows the effects of reheating temperatures and cooling rates on the strength of weld metal after tempering at 550 ℃. After reheating and tempering, the weld metals have high strength. With the increase of reheating temperature and cooling rate, the strength increases. All strength ($R_{t0.5}$) values obtained under any processing conditions are higher than the standard value of 555 MPa. The weld seam of the bends is reinforced, which can assure that the strength of the weld seam is higher than that of the pipe body. Therefore, strength is not a key issue for X80 bends.

Fig. 3 shows the effects of reheating temperature and cooling rate on low-temperature Charpy impact energy. The rules of the influence of reheating temperature on impact energy differ from those of strength. Reheating temperature of 990 ℃ is considered suitable. When the bending temperature is below 990 ℃, the impact energy increases with the increase of bending temperature; when the bending tem-

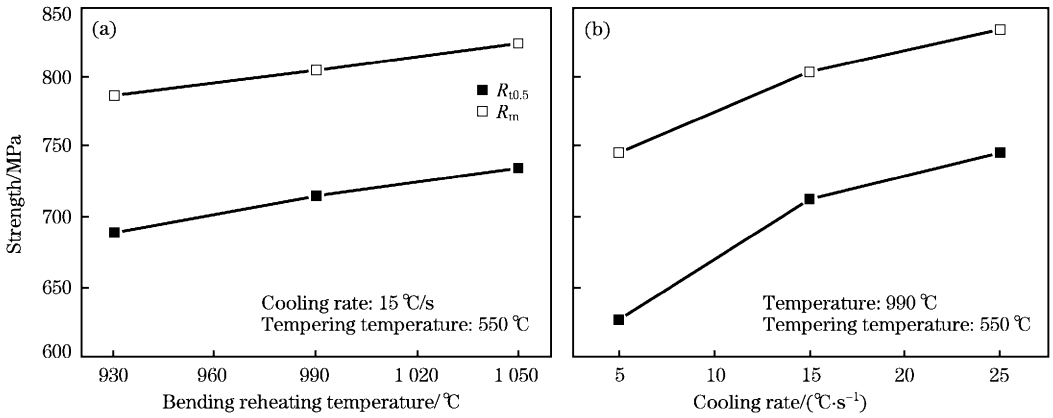

Fig. 2 Effects of bending reheating temperature (a) and cooling rate (b) on strength of weld metal

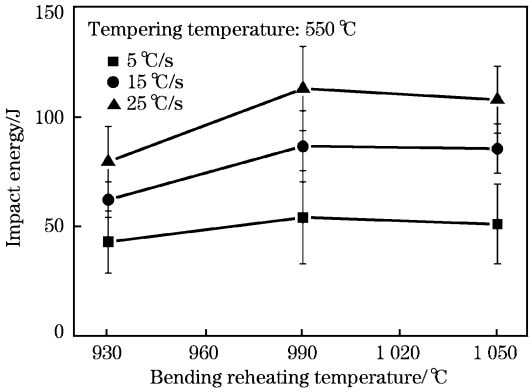

Fig. 3 Effects of reheating temperature on impact toughness of weld metal tested at −20 ℃

perature is over 990 ℃, the impact energy decreases with the increase of bending temperature. Cooling rate also has a great effect on impact energy. With the increase of cooling rate, the values of impact energy increase obviously. When the cooling rate is 5 ℃/s and the reheating temperature is 930 ℃, the impact energy is lower than the critical single value of 50 J and the average value of 75 J. Low-temperature impact toughness is therefore a key issue in manufacturing X80 bends, so that reasonable process parameters must be chosen. The above-mentioned results were obtained only at tempering temperature of 550 ℃. Tempering, as the last working process, determines the final mechanical properties; therefore, the effect of tempering on low-temperature impact toughness of weld metal with X80 bends should be considered.

Fig. 4 shows the effects of tempering temperatures on low-temperature impact toughness of weld metal after reheating at different temperatures and cooling at 15 ℃/s. The weld metal has high impact energy values when the temperature is 500 ℃, and all impact energy values are higher than the critical standard value. When the tempering temperature increased to 550 ℃, the impact energy decreases obviously. The decrease in impact energy becomes gradual with the increase of tempering temperature. Fig. 4 also shows that the weld metal has high impact energy when the reheating temperature is 990 ℃ and the tempering is conducted at any temperature. These results indicate that weld metal needs suitable reheating temperature, cooling rate, and lower tempering temperature to improve the low-temperature impact toughness. The process parameter results are different from those in previous study for bend bodies[9], which is attributed to the different characteristics of change in microstructure of weld metal during reheating and water cooling.

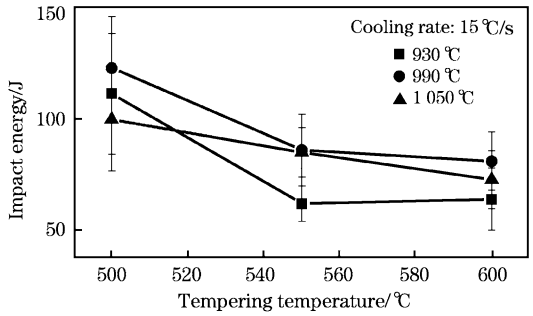

Fig. 4 Effects of tempering temperature on impact energy of the weld metal tested at −20 ℃

2.2 Effects of hot bending parameters on microstructures

Fig. 5 shows SEM microstructures of weld metals after simulating under different reheating and cooling conditions. Although all specimens are tempered at 550 ℃, the optical microstructures still remain the characteristic of direct cooling microstructure; some acicular ferrite and granular bainite can be

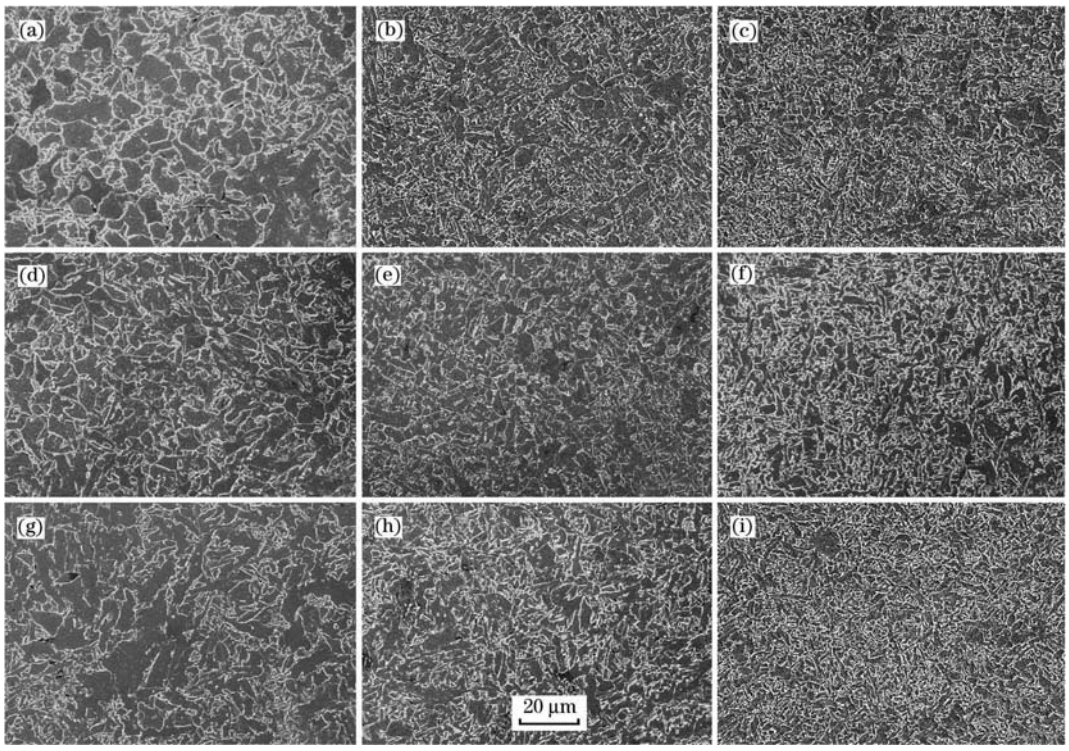

(a) 930 ℃, 5 ℃/s; (b) 930 ℃, 15 ℃/s; (c) 930 ℃, 25 ℃/s; (d) 990 ℃, 5 ℃/s; (e) 990 ℃, 15 ℃/s; (f) 990 ℃, 25 ℃/s; (g) 1050 ℃, 5 ℃/s; (h) 1050 ℃, 15 ℃/s; (i) 1050 ℃, 25 ℃/s.

Fig. 5 SEM micrographs of weld metal with different reheating temperatures and cooling rates tempered at 500 ℃

observed clearly. However, the reheating temperature and cooling rate have great effects on microstructures. At low reheating temperature and cooling rate, the microstructure mainly consists of polygonal ferrite and tempered bainite and the size of ferrite is large (Fig. 5(a)), which decreases strength and impact toughness (Figs. 2 — 4). With the increase of cooling rate and reheating temperature, the microstructures become finer and mainly consist of acicular ferrite and bainite (Fig. 5), which increase strength and impact toughness. When the reheating temperature is over 990 ℃, the microstructures show a coarsening trend with the increase of reheating temperature. Consequently, the impact toughness decreases. With the increase of tempering temperature ranging from 500 to 600 ℃, the acicular ferrite microstructure characteristic weakens, which decreases impact toughness.

2.3 CCT diagrams of weld metal

To understand clearly the difference of microstructure transformation between weld metal and base metal during cooling, CCT diagrams were constructed by dilatation method and microstructure observation. Fig. 6 shows the CCT diagrams, and Fig. 7 shows the microstructures at different cooling rates. The CCT diagrams of the weld metal mainly consist of two-phase transformation fields, i. e., acicular ferrite, bainite and polygonal ferrite, in contrast to those of base metal[9]. The hardenability decreases remarkably, and the critical cooling rate of the polygonal ferrite is 25 ℃/s, which may be attributed to the chemical composition inhomogeneity and nonmetallic oxide inclusions in the weld metal[7,10,11].

Fig. 7(a) shows that when the cooling rate is below 1 ℃/s, the microstructure mainly consists of polygonal ferrite with a little acicular ferrite, bainite,

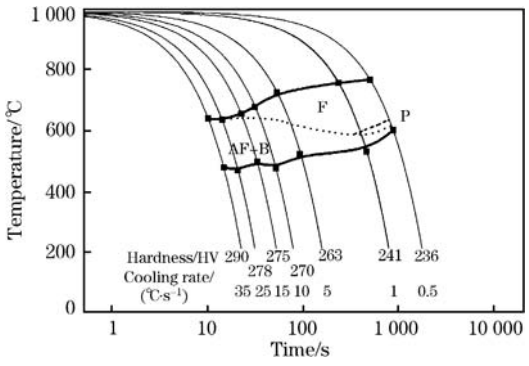

Fig. 6 Continuous cooling transformation diagram of the weld metal

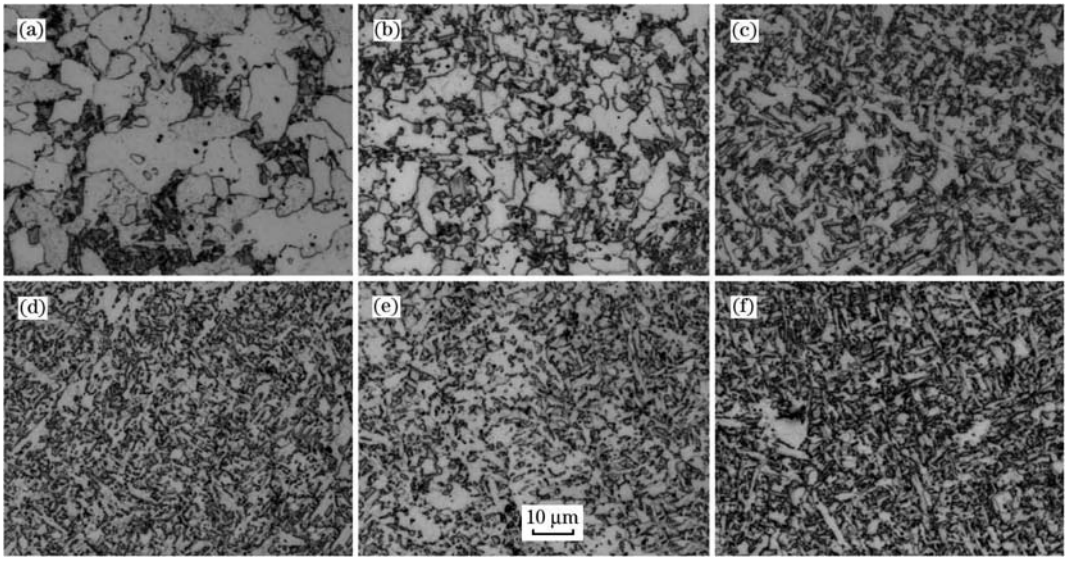

(a) 1 ℃/s; (b) 5 ℃/s; (c) 10 ℃/s; (d) 15 ℃/s; (e) 25 ℃/s; (f) 35 ℃/s.

Fig. 7 Optical micrographs of weld metal after direct cooling with different cooling rates

and pearlite distributed at the intersection of the polygonal ferrite grains. Meanwhile, some fine black dot second-phase particles distributed in ferrite grain can be observed. Such particles may be non-metallic oxide inclusions formed during welding[7,10,11] or polygonal ferrite nuclear cores accelerating the polygonal ferrite transformation[11]. As SEM revealed (Fig. 8(a)), polygonal ferrite grows around a non-metallic oxide inclusion particle. The microstructure transformed at high temperature possesses low strength (Fig. 9). When the cooling rate increased to 5 ℃, the microstructure mainly consists of polygonal ferrite

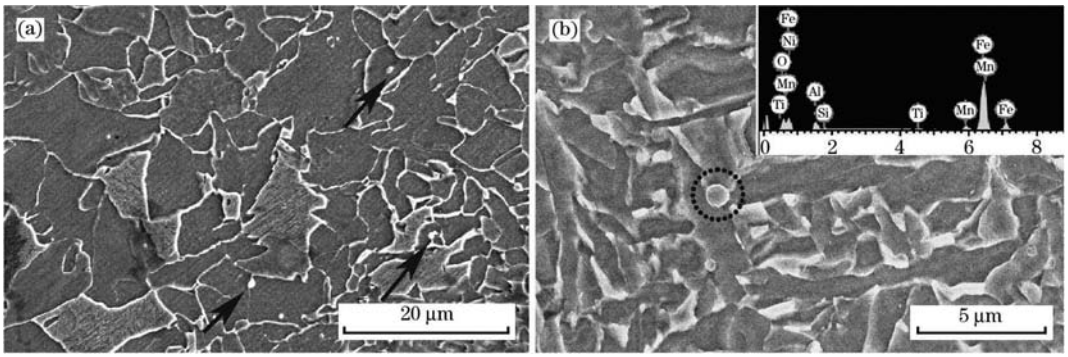

Fig. 8 Effects of non-metallic oxide inclusions on nucleation of polygonal ferrite (a) and intragranular acicular ferrite (b)

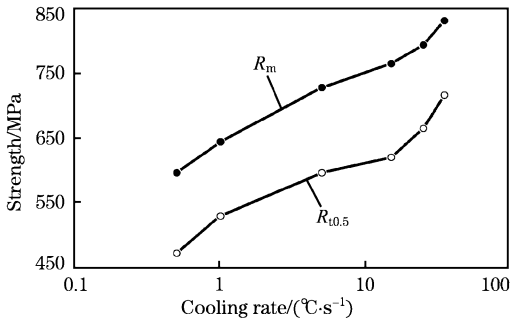

Fig. 9 Effects of cooling rate on strength of weld metal reheated at 990 ℃

with acicular ferrite and bainite but pearlite cannot be observed (Fig. 7(b)). The yield strength is 597 MPa (Fig. 9), which is higher than the critical value of 555 MPa. The results indicate that the strength can meet the standard requirements when the cooling rate is over 5 ℃/s.

When the cooling rate is 10 ℃/s, the microstructure is dominated by acicular ferrite and bainite; the acicular ferrites have short and thick acicular shapes and an overlapping trait (Fig. 7(c)), because the non-metallic oxide inclusions promote the nucle-

ation of acicular ferrite in austenite grain (Fig. 8 (b)). The overlapping acicular ferrites will improve strength and toughness[10,11].

When the cooling rate increased to over 15 ℃/s, the microstructure is refined remarkably and the amount and length-width ratio of acicular ferrite increase, which is similar to the microstructure of weld metal after direct welding (Fig. 7(d)). Meanwhile, some large-sized polygonal ferrites distributed along prior dendrite can be observed in the microstructure, even when the cooling rate is increased to 25 ℃/s (Fig. 7 (e)). When the cooling rate is increased to 35 ℃/s, the size of acicular ferrite decreases and the amount of dot-like island constituent increases (Fig. 7(f)). The refined overlapping acicular ferrite and bainite microstructures result in increased strength and toughness (Fig. 9).

3 Discussion

According to the results stated above, the variation in mechanical properties of weld metal with the reheating temperature (Figs. 2(a) and 3) is similar to that of base metal[9], e. g., with the increase of heating temperature, the strength increases (Fig. 2(a)), and the highest low-temperature impact energy appears at 990 ℃ (Fig. 3). However, the effects of the cooling rate and tempering temperature differ from the common rules of tempering for pipeline steels, e. g., the strength and impact toughness increase with the increase of cooling rate (Figs. 2(b) and 3), and with the increase of tempering temperature, the impact toughness decreases (Fig. 4). Such differences are attributed to the non-metallic oxide inclusions existed in weld metal, which can be the nucleuses of the polygonal ferrite and/or acicular ferrite (Fig. 8), affecting the microstructure transformation during reheating and tempering and the final microstructure and mechanical properties of the bends.

At lower heating temperature and cooling rate, large sizes of polygonal ferrite and massive ferrite are obtained (Figs. 5 and 7), which show low strength and impact toughness at the same temperature (Figs. 2—4). With the increase of heating temperature and cooling rate, the amount of overlapping acicular ferrite increases. The overlapping acicular ferrite nucleated from non-metallic inclusion is considered a key reason for obtaining high impact toughness and strength[10—14]. With increasing the heating temperature over 990 ℃, the prior austenite gain coarsens and the amount of bainite increases (Fig. 5); consequently, the strength increases, whereas the impact toughness decreases (Figs. 2 and 4).

The variation in acicular ferrite microstructure of weld metal with the tempering temperature differs from the general pipeline steels, i. e., the strength increases with the increase of tempering temperature, whereas the low-temperature impact toughness decreases (Fig. 4). The overlapping acicular ferrite of the weld metal obtained after heating and direct water cooling (Fig. 10(a)) is considered to have high impact toughness and strength[10—14], whereas the microstructure degrades (Fig. 7) after tempering, which decrease the impact toughness. Although the M/A constituents decompose to carbide and ferrite, which improve the impact toughness, fine NbC and/or VC particles precipitate in ferrite matrix (Fig. 10(b)), which increases the strength and decreases the impact toughness. As shown in the CCT

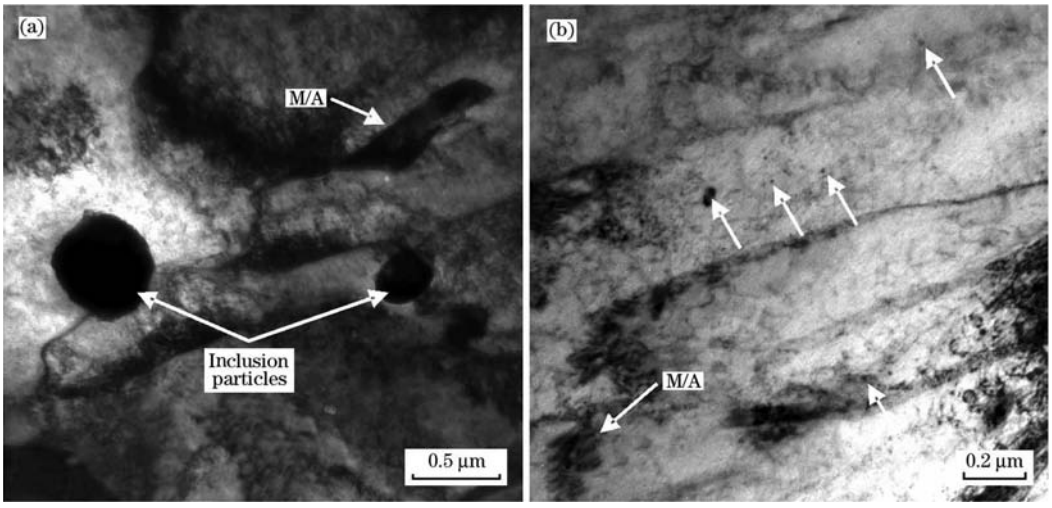

Fig. 10 TEM microstructures of directly cooled sample after reheating at 990 ℃ and cooling with 15 ℃/s (a) and the sample tempered at 550 ℃/s (b)

diagrams, the transformed temperature of acicular ferrite ranges from approximately 470 to 640 ℃ (Fig. 6); therefore, the degeneration degree of the acicular ferrite increases with the increase of temperature, and the amount and size of the NbC and/or VC precipitate particles increase. These factors result in decreased impact toughness. To obtain high impact toughness, the optimum reheating temperature is approximately 990 ℃ and tempering should be conducted at low temperature. For heavy-wall X80 bends, the optimum reheating parameter design should consider the balance of strength and toughness of weld and base metals.

4 Conclusions

(1) During the manufacturing of heavy-wall X80 hot bends, the strength of the weld metal has a value of 555 MPa specified in the technical specification under practical manufacturing process conditions. With the increase of reheating temperature, cooling rate, and tempering temperature, the strength increases. The impact toughness shows an apparent relation to the variation in reheating and tempering temperatures. When the reheating temperature is 990 ℃ and the tempering is conducted at lower temperature, the weld metal can obtain high impact toughness. Therefore, for the weld metal with heavy-wall X80 hot introduction bends, opportune reheating temperature and low tempering temperature should be considered to ensure high impact toughness.

(2) The overlapping acicular ferrite-like as-welded state obtained after direct cooling from reheating temperature generates weld metal with high strength and toughness. The degeneration of the overlapping acicular ferrite during tempering decreases strength and toughness. By contrast, the NbC and VC precipitation during reheating and tempering increases strength but decreases toughness.

References:

[1] A. Mannucci, E. Anelli, F. Zana, T. Claudio, A. Mariano, A. Laura, P. Giorgio, in: C. C. Mei (eds.), Proceedings of the International Conference on Offshore Mechanics and Arctic Engineering 2009, Volume 6: Materials Technology, American Society of Mechanical Engineers, New York, 2009, pp. 175-185.

[2] G. Z. Batista, H. Eduardo Jr., N. Leonardo, I. S. De Bott, in: Proceedings of the ASME International Pipeline Conference 2006, IPC 2006, 3 (PART A), American Society of Mechanical Engineers, New York, 2007, pp. 89-98.

[3] S. J. Jia, L. N. Duan, Q. Y. Liu, Trans. Mater. Heat Treat. 33 (2012) 76-81.

[4] C. J. Shang, X. D. Li, W. J. Nie, D. X. Xia, S. J. Wu, In: Materials Science and Technology Conference and Exhibition 2012, MS and T 2012, Association for Iron and Steel Technology, Warrendale, 2012, pp. 904-916.

[5] R. A. Silva, G. Z. Batista, L. F. G. De Souza, I. S. Bott, Mater. Sci. Forum. 706-709 (2012) 2059-2065.

[6] E. Muthmann, W. Kaluza, M. Liedke, W. Scheller, in: Pipeline Technology Conference, Ostend, Belgium, 2009, pp. 211-215.

[7] B. Beidokhti, A. H. Koukabi, A. Dolati, J. Mater. Process. Technol. 209 (2009) 4027-4035.

[8] P. C. Chung, Y. J. Ham, S. H. Kim, J. H. Lim, C. H. Lee, Mater. Des. 34 (2012) 685-690.

[9] X. Wang, F. R. Xiao, Y. H. Fu, X. W. Chen, B. Liao, Mater. Sci. Eng. A 530 (2011) 539-547.

[10] D. L. Ren, F. R Xiao, P. Tian, X. Wang, B. Liao, Int. J. Miner. Metall. Mater. 16 (2009) 65-70.

[11] B. Kim, S. Uhm, C. Lee, J. B. Lee, Y. H. An, J. Eng. Mater. Technol. Trans. ASME 172 (2005) 204-213.

[12] J. Zachrisson, J. Borjesson, L. Karlsson, Sci. Technol. Weld. Joining 18 (2013) 603-609.

[13] A. S. Oryshchenko, A. V. Pimenov, S. I. Shekin, M. G. Sharapov, Weld. Int. 27 (2013) 681-686.

[14] S. P. Lu, S. T. Wei, D. Z. Li, Y. Y. Li, J. Mater. Sci. 45 (2010) 2390-2402.